Preprints of the 21st IFAC World Congress (Virtual)
Berlin, Germany, July 12-17, 2020

A New Robust Command Shaping Method and Its Application in Quadrotor Slung System with Varying Parameters ⋆

Chenxing Li [*,**] **Xin Huo** [**] **Qingquan Liu** [**]

[*] *Department of Informatics, Technical University of Munich, Munich, CO 85716, Germany (e-mail: chenxing.li@tum.de)*
[**] *Control and Simulation Center, Harbin Institute of Technology, Harbin 150080, China (e-mail: huoxin@hit.edu.cn)*

Abstract: Command shaping method is a mature feedforward control approach, and there exist many successful applications in the industrial fields. However, the traditional instruction shapers either are sensitive to the system parameters, or have some robustness but difficult to adjust the parameters, and meanwhile their conservations are increased unsurprisingly. To this end, a new robust command shaper is proposed in this paper, which is inspired by the two-mode ZV shaper and the EI shaper. The theoretical design procedure of the new shaper is presented. Besides, the robustness of the new shaper is analyzed and compared with other shapers based on the sensitivity curve. Finally, the shaper proposed in this paper is applied to the quadrotor slung system with varying parameters, and its effectiveness and superiority are proved by numerical simulations and comparative analyses.

Keywords: Command Shaper, Quadrotor Slung System, Vibration Suppression, Robustness, Modeling Error

1. INTRODUCTION

The quadrotor is a new type of air transport vehicle which has the potential to hover and take off, fly and land in small areas, cf.: Mellinger et al. (2011). Now, the quadrotor is widely used in military and civil applications, such as material delivery and logistics, etc. In modern logistic industry, the quadrotor trends to be used to transport some packages since transportation on road is almost saturated. Sometimes it is necessary to use quadrotor to share the transportation volume during the rush hours. Amazon, Google and S. F. Express have carried out UAV Express projects in remote areas such as Fig. 1. However, due to the lack of stability and reliability of transportation, the applications are limited. Therefore, it is necessary to solve these problems caused by payload vibration.

Different control methods have been proposed to control the quadrotor since the slung system significantly alters the flight characteristics of the quadrotor. These methods are divided into feedback and feed-forward control, cf.: Sadr et al. (2014), Haddadi et al. (2015). Feedback control methods use measurements and estimations of system states to reduce the vibration while feed-forward control methods change actuator commands for reducing the vibration. The feed-forward controller can improve the performance of feedback controller. Thus, proposing feed-forward algorithms can lead to more practical and accurate control of these systems, cf.: Njeri and Matsushita (2018). One effective feed-forward method is the command shaping theory.

Fig. 1. Quadrotor slung system with swing payload

Command shaper is realized by convoluting a sequence of impulses with desired instructions to generate an appropriate reference command. Creating special reference commands to move flexible systems without vibration is a traditional idea, cf.: Singhose (2009) and references therein. The early form of command shaper was posicast control, which is the prototype of Zero Vibration (ZV) shaper put forward by Smith (1957). It solves the problem of vibration suppression at natural frequency of system. Unfortunately, we will never know the system parameters perfectly, so we cannot assume that redesigning the command shaper is always an optimal option. Furthermore, the parameters are likely to change somewhat over time or during the motion. What is needed is a robust command shaper that works well even when there are modeling

⋆ This work was supported by the National Natural Science Foundation of China under Grants 61773138 and 61427809.(Corresponding author: Xin Huo.)

errors. This robustness problem was first solved by Singer and Seering (1990) by adding additional constraint on the derivative of residual vibration magnitudes, which results in Zero Vibration and Derivative (ZVD) shaper. On the basis of ZVD, Zero Vibration Double Derivative (ZVDD) was proposed by Singer and Seering (1990) to further enhance the robustness. Another shaper put forward by Ingram and Chiu (2002) of increasing robustness is to relax zero vibration constraints at natural frequency, such as Extra-Insensitive (EI) shaper, which has more robustness by sacrificing the accuracy at the natural frequency.

Although these command shapers are widely used in industry, cf,: Auernig and Troger (1987), Kim and Singhose (2010), Adams et al. (2015), they still have some disadvantages. The delay of ZV is the smallest, but its robustness is too poor to be used in practice. ZVDD has the best robustness, but its large delay is easy to cause stability problems. EI and ZVD have the same appropriate delay, however, the robustness of ZVD is not strong enough, while EI has poor design flexibility and high computational complexity. They more or less have some limitations. The purpose of this paper is to investigate a new command shaper that will cause the systems to complete desired moves robustly and accurately.

The rest of the paper is organized as follows. Section 2 reviews the basic definitions and typical command shaping methods. The main results are presented in Section 3, where the new robust command shaper is proposed, and its robustness and accuracy are analyzed and compared with the traditional ones. An example of quadrotor slung system with varying parameters is investigated in Section 4, where the effectiveness and the superiority in vibration suppression of the swing payload are illustrated by simulation comparison. Section 5 summaries the whole paper.

2. PRELIMINARIES

In this section, some typical command shaping methods are reviewed. For the sake of brevity, we denote by $\mathcal{C}$ and $\mathcal{S}$ the cosine and sine functions throughout the paper.

2.1 Residual Vibration

A mathematical description of the residual vibration that results from an impulse sequence can be described by

$$V(\omega_n, \xi) = e^{-\xi\omega_n t_n}\sqrt{[C(\omega_n, \xi)]^2 + [S(\omega_n, \xi)]^2} \quad (1)$$

where

$$C(\omega_n, \xi) = \Sigma_{i=1}^{n} A_i e^{\xi\omega_n t_i}\mathcal{C}(\omega_d t_i) \quad (2)$$

and

$$S(\omega_n, \xi) = \Sigma_{i=1}^{n} A_i e^{\xi\omega_n t_i}\mathcal{S}(\omega_d t_i) \quad (3)$$

where $V \in [0, 1]$ is the residual vibration, $\xi \in (0, 1)$ is damping ratio, ω_n is undamped natural frequency of the system. A_i and $t_i, i = 1, \ldots, n$ are the amplitudes and time locations of the impulses, n is the number of impulses in the sequence, cf.: Singhose and Seering (2011). The damped natural frequency is

$$\omega_d = \omega_n\sqrt{1 - \xi^2} \quad (4)$$

Without loss of generality, we can set the time location of the first impulse equals to zero, i.e., $t_1 = 0$. To generate an impulse sequence that causes no residual vibration, the following restrictions should be satisfied

$$V(\omega_n, \xi) = 0 \quad (5)$$

and

$$\Sigma_{i=1}^{n} A_i = 1 \quad (6)$$

where $A_i > 0, i = 1, \ldots, n$ aims to avoid the trivial solution of all zero-valued impulses and to obtain a normalized and bounded result.

2.2 Typical Command Shapers

If the accurate system model is available, the sequence of two impulses that leads to Zero Vibration (ZV) shaper can be stated in matrix form as

$$\begin{bmatrix} A_i \\ t_i \end{bmatrix} = \begin{bmatrix} \frac{1}{1+K} & \frac{K}{1+K} \\ 0 & 0.5T_d \end{bmatrix} \quad (7)$$

where

$$K = e^{\frac{\xi\pi}{\sqrt{1-\xi^2}}} \quad (8)$$

and

$$T_d = \frac{2\pi}{\omega_d} \quad (9)$$

A ZV shaper is based on the assumption that an accurate model of the plant dynamics exists. However, this assumption is not always the case in practice. The first command shaper designed to have robustness to modeling errors is Zero Vibration and Derivative (ZVD) shaper. This shaper is designed by requiring the partial derivative of the residual vibration equals to zero at the modeling frequency. Mathematically, this can be stated as

$$\frac{\partial V(\omega, \xi)}{\partial \omega} = 0 \quad (10)$$

The ZVD shaper is obtained by

$$\begin{bmatrix} A_i \\ t_i \end{bmatrix} = \begin{bmatrix} \frac{1}{(1+K)^2} & \frac{2K}{(1+K)^2} & \frac{K^2}{(1+K)^2} \\ 0 & 0.5T_d & T_d \end{bmatrix} \quad (11)$$

Actually, forcing the command to produce exactly zero vibration at the modeling frequency is not a particularly useful design constraint in the case that there exists a fair amount of uncertainty. An Extra-Insensitive (EI) shaper is proposed which simply constrains the residual vibration at some tolerable level, so that more robustness can be obtained without incurring additional time delay. The impulse sequence of an EI shaper is

$$\begin{bmatrix} A_i \\ t_i \end{bmatrix} = \begin{bmatrix} \frac{1+V_{tol}}{4} & \frac{1-V_{tol}}{2} & \frac{1+V_{tol}}{4} \\ 0 & 0.5T_d & T_d \end{bmatrix} \quad (12)$$

where V_{tol} is the tolerable limit on percentage residual vibration, cf.: Singhose and Seering (2011).

2.3 Sensitivity Curve

The robustness of a command shaper can be visualized by plotting its sensitivity curve, which shows the residual vibration after an impulse sequence is added to the system. The sensitivity curves for the ZV, ZVD and EI shapers are demonstrated in Fig. 2, where the horizonal axis is a normalized frequency, i.e., ω and ω_d denote the actual frequency and the modeling frequency, respectively, and

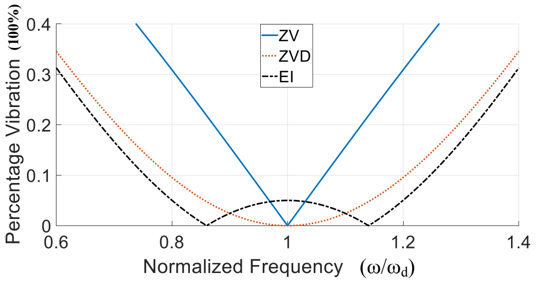

Fig. 2. Sensitivity curves of ZV, ZVD and EI shapers

the percentage vibration as defined in (1) is plotted on the vertical axis.

The robustness of a command shaper can be quantitatively evaluated by the width of its sensitivity curve at certain tolerable vibration level, as shown in Fig. 2. In this case, the 5% insensitivity of the EI shaper is larger than the ZVD shaper, both of which are far larger than the ZV shaper. That means, the ZV shaper provides perfect vibration suppression at a specific frequency, but the amount of vibration increased rapidly considering the perturbation of model parameters.

3. MAIN RESULTS

Compared with the ZV shaper, a ZVD shaper is more robust which relaxes the necessary of the accurate system model. However, their robustness is not strong enough which results in other types of shapers such as the two-mode ZV and the EI shaper. A two-mode ZV shaper eliminates the vibration at two frequency points by convolving two ZV shapers, but the maximum vibration between the two frequency points is not considered. An EI shaper utilizes V_{tol} to restrict the tolerable limit of the vibration, but its amplitudes and time locations of impulses are coupled with V_{tol} and ω_d, which causes a huge computational complexity, cf.: Singhose and Seering (2011).

Inspired by the two-mode ZV and EI shaper, a new command shaping method is proposed in this section. It is called Virtual Insensitive (VI) shaper, which causes systems to complete desired moves robustly and accurately.

3.1 Configuration of the New Shaper

Assume ω_1 and ω_2 are the virtual frequency points which locates on the left and right side of ω_d, respectively. Without loss of generality, assume $\omega_1 \leq \omega_d \leq \omega_2$. Based on the two-mode ZV shaper, it is necessary to combine the qualities of the two shapers by convolving them, which leads to an impulse sequence with four impulses. In the sequel, the amplitude and time location of the impulses should be determined, respectively.

(1) Amplitudes of the impulses

The amplitudes of the impulses should suppress vibrations at ω_1 and ω_2, so that

$$V(w_1, \xi) = V(w_2, \xi) = 0 \tag{13}$$

which means

$$\Sigma_{i=1}^{4} A_i e^{\xi \omega_j t_i} \mathcal{C}(\omega_j t_i) = 0 \tag{14}$$

$$\Sigma_{i=1}^{4} A_i e^{\xi \omega_j t_i} \mathcal{S}(\omega_j t_i) = 0 \tag{15}$$

where $j = 1, 2$. By solving (14) and (15), the amplitudes of the impulses can be derived as

$$K^2 A_1 = K A_2 = K A_3 = A_4 \tag{16}$$

If damping is ignored, i.e., let $\xi = 0$, the amplitudes of the impulses can be obtained as

$$A_i = 0.25, \ i = 1, 2, 3, 4 \tag{17}$$

(2) Time locations of the impulses

According to (1) and (17), the relation between the residual vibration and the natural frequency is represented as

$$\begin{aligned} V^2 = \ & \Sigma_{i=1}^{4} A_i^2 + 2A_3A_4\mathcal{C}(\omega t_2) + 2A_1A_2\mathcal{C}(\omega t_2) \\ & + 2A_1A_3\mathcal{C}(\omega t_3) + 2A_1A_4\mathcal{C}(\omega t_4) \\ & + 2A_2A_4\mathcal{C}(\omega t_3) + 2A_2A_3\mathcal{C}[\omega(t_3 - t_2)] \end{aligned} \tag{18}$$

which can be simplified as follows,

$$V = |\mathcal{C}(\frac{\omega t_2}{2}) \cdot \mathcal{C}(\frac{\omega t_3}{2})| \tag{19}$$

Based on the EI shaper, V reaches its maximum V_{max} when $\omega = \omega_d$. If V_{tol} is given, the system could meet the requirements of the maximum vibration by guaranteeing $V_{max} \leq V_{tol}$,

$$V_{max} = |\mathcal{C}(\frac{\omega_d t_2}{2}) \cdot \mathcal{C}(\frac{\omega_d t_3}{2})| \leq V_{tol} \tag{20}$$

The design idea of the new VI shaper is that, if ω_d and V_{tol} are given, an appropriate virtual frequency ω_1 on the left side of ω_d can be selected, then the range of ω_2 can be obtained by (20) on the right side of ω_d, and vice versa. Thus, the time locations of impulses can be expressed as

$$t_1 = 0, \ t_2 = 0.5T_{d2}, \ t_3 = 0.5T_{d1}, \ t_4 = t_2 + t_3 \tag{21}$$

where $T_{d1} = \frac{2\pi}{\omega_1}$ and $T_{d2} = \frac{2\pi}{\omega_2}$ are the virtual vibration periods, respectively. Finally, the matrix form of the impulse sequence with a VI shaper can be formulated as

$$\begin{bmatrix} A_i \\ t_i \end{bmatrix} = \begin{bmatrix} 0.25 & 0.25 & 0.25 & 0.25 \\ 0 & 0.5T_{d2} & 0.5T_{d1} & 0.5(T_{d1} + T_{d2}) \end{bmatrix} \tag{22}$$

3.2 Robustness Analysis

The sensitive curve of the new VI shaper is shown in Fig. 3, together with the well-developed ZV, ZVD and EI shapers. Obviously, it has a wider width of its sensitivity curve at 5% tolerable vibration level, which demonstrates a significant robustness compared with the traditional shaper. It should be noted that the robustness of a VI shaper is at the same level compared with the EI shaper in the case that they have the same V_{tol} on ω_d.

Remark 1 Analogous to the ZVD and EI shaper, the VI shaper has one vibration period, which is twice of the ZV shaper. However, a substantial amount of robustness is obtained for this small increase in time delay.

3.3 Accuracy Comparison with EI Shaper

For an EI shaper, when ω_d and V_{tol} are given, the impulse sequence can be designed by (12). However, when ω_d changes, the time locations can be redesigned according to the change, while the amplitudes cannot be changed easily since V_{tol} after change is cannot be known, which means $V_{max} = V_{tol}$ remaining unchanged after ω_d changed.

For a VI shaper, ω_1 or ω_2 is set roughly on the left and right side of ω_d for a VI shaper. If one of them is fixed, the other

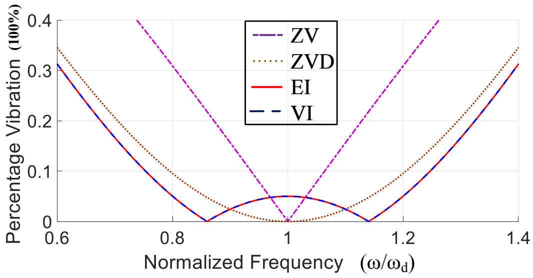

Fig. 3. Sensitivity curves of ZV, ZVD, EI and VI shapers

can be calculated the range by solving (20). Therefore, the turning of the VI shaper is more convenient than the EI shaper. More importantly, V_{max} of a VI shaper will decrease after turning when the parameters of the system change, which is illustrated below.

Theorem 1. For a VI shaper, the maximum vibration V_{max} will decrease from the initial tolerable vibration level V_{tol} if the virtual left-side frequency ω_1 increases or the virtual right-side frequency ω_2 decreases within their limits.

Proof. If $\omega_1 \leq \omega \leq \omega_2$, V in (19) is negative, which can be expressed as

$$V = -\mathcal{C}(\frac{\omega t_2}{2}) \cdot \mathcal{C}(\frac{\omega t_3}{2}) \quad (23)$$

The partial derivative of V about ω is

$$\frac{\partial V}{\partial \omega} = \frac{1}{2}[t_3 \mathcal{S}(\frac{\omega t_3}{2}) \cdot \mathcal{C}(\frac{\omega t_2}{2}) + t_2 \mathcal{S}(\frac{\omega t_2}{2}) \cdot \mathcal{C}(\frac{\omega t_3}{2})] \quad (24)$$

Let $\frac{\partial V}{\partial \omega} = 0$, V reaches its maximum value which satisfies

$$t_3 \tan(\frac{\omega t_3}{2}) + t_2 \tan(\frac{\omega t_2}{2}) = 0 \quad (25)$$

Thus V_{max} can be expressed as

$$V_{max} = -\mathcal{C}(\frac{\omega^* t_3}{2}) \cdot \mathcal{C}(\frac{\omega^* t_2}{2}) \quad (26)$$

where ω^* is the extreme point which makes $V = V_{max}$.

Considering the relationship between V_{max} and virtual frequency ω_1 and ω_2, it is necessary to treat V_{max} as a variable, and to obtain partial derivative for t_2 and t_3, which is related with ω_1 and ω_2, that is

$$\frac{\partial V_{max}}{\partial t_3} = \frac{\omega^*}{2} \mathcal{S}(\frac{\omega^* t_3}{2}) \cdot \mathcal{C}(\frac{\omega^* t_2}{2}) \quad (27)$$

$$\frac{\partial V_{max}}{\partial t_2} = \frac{\omega^*}{2} \mathcal{C}(\frac{\omega^* t_3}{2}) \cdot \mathcal{S}(\frac{\omega^* t_2}{2}) \quad (28)$$

Considering that

$$\mathcal{C}(\frac{\omega^* t_2}{2}) > 0, \ \mathcal{S}(\frac{\omega^* t_3}{2}) > 0 \quad (29)$$

$$\mathcal{C}(\frac{\omega^* t_3}{2}) < 0, \ \mathcal{S}(\frac{\omega^* t_2}{2}) > 0 \quad (30)$$

According to (29) and (30), it is obvious that if ω_1 increases, V_{max} will decrease. Analogously, if ω_2 decreases, V_{max} will decrease too. Since we started our design at certain tolerable vibration level V_{tol}, thus we derive that the maximum vibration $V_{max} \leq V_{tol}$.

Remark 2 Compared with the EI shaper, the impulses sequence of a VI shaper is no longer coupled with V_{tol} and ω_d, so that the parameters of the shaper have good design flexibility. Furthermore, V_{max} is less than the initial V_{tol} after turning the shaper due to the change of parameters, which means the VI shaper has a higher accuracy.

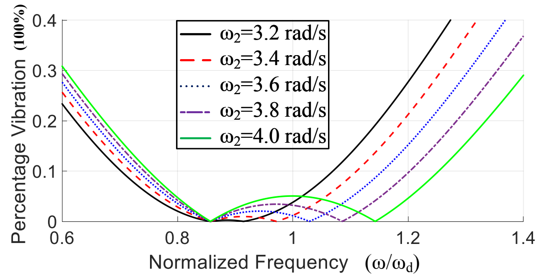

Fig. 4. Sensitivity curves under changed ω_2

Fig. 4 shows the change of V_{max} when ω_d is changing from 3.5 rad/s to 3.1 rad/s. In this process, $\omega_1 = 3$ rad/s remains unchanged while ω_2 is changed at specific values.

4. CASE STUDIES AND COMPARISONS

In this section, an example of quadrotor slung system with varying parameters will be investigated to test and verify the robustness and accuracy of the VI shaper. The following assumptions are considered for the sake of brevity: (1) The quadrotor is rigid and symmetrical; (2) Distribution of mass is uniform; (3) The suspension point of the payload is the geometric center of the quadrotor, which is also the point of gravity. The definition of coordinate system is shown in Fig. 5, and see Huo et al. (2019) for the coordinate transformation and the detailed information.

4.1 Quadrotor Slung System

The Lagrangian Equations can be described as

$$\frac{\mathrm{d}}{\mathrm{d}t}(\frac{\partial \Lambda}{\partial \dot{\rho}}) - \frac{\partial \Lambda}{\partial \rho} = 0 \quad (31)$$

where ρ is the variable that we concern, Λ is Lagrangian operator which equals to kinetic energy minus potential energy.

Considering the influence of the payload on the quadrotor body, the translation model of the quadrotor body can be expressed as follows,

$$\begin{cases} \ddot{x} = \dfrac{\mathcal{S}\psi\mathcal{S}\phi + \mathcal{S}\theta\mathcal{C}\psi\mathcal{C}\phi}{M+m}\Sigma_{i=1}^{4} F_i - \dfrac{m}{M+m}\ddot{p} \\ \ddot{y} = \dfrac{-\mathcal{C}\psi\mathcal{S}\phi + \mathcal{S}\theta\mathcal{S}\psi\mathcal{C}\phi}{M+m}\Sigma_{i=1}^{4} F_i - \dfrac{m}{M+m}\ddot{q} \\ \ddot{z} = -\dfrac{\mathcal{C}\theta\mathcal{C}\phi}{M+m}\Sigma_{i=1}^{4} F_i + \dfrac{m}{M+m}\dfrac{(\dot{p}p + \dot{q}q)^2}{r^3} \\ \quad + \dfrac{m}{M+m}\dfrac{\dot{p}^2 + \dot{q}^2 + \ddot{p}p + \ddot{q}q}{r} + \dfrac{mg\frac{r}{L} + Mg}{M+m} \end{cases} \quad (32)$$

The rotation model can be expressed as

$$\begin{cases} \ddot{\phi} = \dfrac{I_y - I_z}{I_x}\dot{\theta}\dot{\psi} + \dfrac{l}{I_x}(F_4 - F_2) \\ \ddot{\theta} = \dfrac{I_z - I_x}{I_y}\dot{\phi}\dot{\psi} + \dfrac{l}{I_y}(F_1 - F_3) \\ \ddot{\psi} = \dfrac{I_x - I_y}{I_z}\dot{\theta}\dot{\phi} + \dfrac{l}{I_z}(F_1 + F_3 - F_4 - F_2) \end{cases} \quad (33)$$

where x, y, z are the positions to the quadrotor, p, q, r are the relative positions of the payload to the quadrotor. φ,

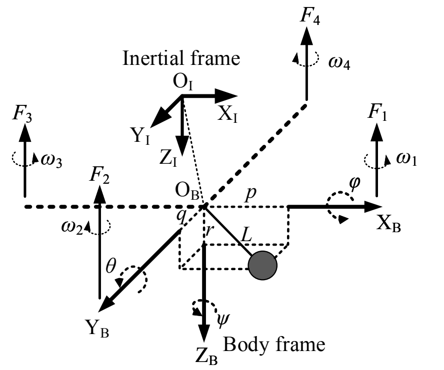

Fig. 5. The quadrotor with one solid sphere payload.

θ, ψ are roll angle, pitch angle and yaw angle, respectively. $\Sigma_{i=1}^{4} F_i = F_1 + F_2 + F_3 + F_4$ is the sum of elevating force provided by the rotors. M is the mass of quadrotor. m is the mass of the payload. l is the distance between the rotor and the center of quadrotor. L is the length of rope. I_x, I_y, I_z are the moment of inertia around the three axes.

From (31), (32) and (33), the motion equation of the payload can be obtained as follows,

$$\begin{cases} \ddot{p} = [r^4\ddot{x} - pr^3\ddot{z} + pqr^2\ddot{q} + (pL^2 - pq^2)\dot{p}^2 + \\ \quad (pL^2 - p^3)\dot{q}^2 + 2q\dot{q}\dot{p}p^2 + pgr^3]/[r^2(q^2 - L^2)] \\ \ddot{q} = [r^4\ddot{y} - qr^3\ddot{z} + pqr^2\ddot{p} + (qL^2 - qp^2)\dot{q}^2 + \\ \quad (qL^2 - q^3)\dot{p}^2 + 2p\dot{q}\dot{p}q^2 + qgr^3]/[r^2(p^2 - L^2)] \\ r = \sqrt{L^2 - p^2 - q^2} \end{cases} \tag{34}$$

4.2 Shaper Design

The quadrotor slung system can be considered as a single pendulum, and the initial system parameters used in the simulation are shown in Table 1. Assuming $\xi = 0$, the natural frequency of the payload is

$$\omega_n = \sqrt{\frac{g}{L}(1 + \frac{m}{M})} = 3.464 \text{ rad/s} \tag{35}$$

A double closed-loop control block diagram with command shaper is used in simulation, as shown in Fig. 6, where a position loop is designed for the quadrotor, and a relative position loop of the payload is added for improving the vibration suppression performance. Also see Huo et al. (2019) for a detailed description of the double closed-loop control strategy. The impulses sequences based on ZV, ZVD, EI and VI are presented as follows, respectively.

The ZV shaper is given as

$$\begin{bmatrix} A_i \\ t_i \end{bmatrix} = \begin{bmatrix} 0.5 & 0.5 \\ 0 & 0.907 \end{bmatrix} \tag{36}$$

The ZVD shaper is designed as

$$\begin{bmatrix} A_i \\ t_i \end{bmatrix} = \begin{bmatrix} 0.25 & 0.5 & 0.25 \\ 0 & 0.907 & 1.814 \end{bmatrix} \tag{37}$$

Consider $V_{tol} = 5\%$ and $T_d = \frac{2\pi}{\omega_n}$, the EI shaper is designed as

$$\begin{bmatrix} A_i \\ t_i \end{bmatrix} = \begin{bmatrix} 0.2625 & 0.475 & 0.2625 \\ 0 & 0.907 & 1.814 \end{bmatrix} \tag{38}$$

Finally, the VI shaper is designed with the same V_{tol}. Here, we select the left-side virtual frequency $\omega_1 = 3$ rad/s, so

Table 1. Initial parameters of the system

Parameter	Symbol	Value
Mass of quadrotor (Kg)	M	1
Mass of payload (Kg)	m	0.2
Length of the rope (m)	L	1
Distance of rotor and quadrotor center (m)	l	0.25

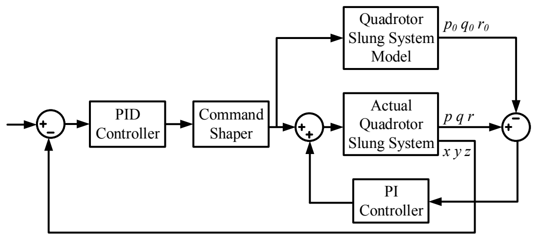

Fig. 6. The control block diagram.

that $\omega_2 = 3.994$ rad/s by solving (20). Thus, the VI shaper can be expressed as

$$\begin{bmatrix} A_i \\ t_i \end{bmatrix} = \begin{bmatrix} 0.25 & 0.25 & 0.25 & 0.25 \\ 0 & 0.7866 & 1.0472 & 1.8338 \end{bmatrix} \tag{39}$$

4.3 Simulation Results

By using the command shaping methods presented above, the simulation results are shown and compared in Figs. 7-11. Fig. 7 shows the comparison result in the case that the accurate parameters of system are known, and it is notable that all of the shapers have obvious effect on restraining the residual vibrations.

However, if L is changed from 1 m to 1.5 m without any prior information, as shown in Fig. 8, the residual vibration of a ZV shaper is far worse than others, since ω_d is changed to 2.828 rad/s. In this case, the EI and VI shapers get the minimal residual vibrations, which means they have better robustness than ZV and ZVD shapers.

The control effect of EI and VI shapers in Fig. 7 is shown in Fig. 9. It can be seen that their control effect is very similar, because when these shapers are built according to the precise model, the VI shaper degenerates into EI shaper to some extent. However, the shaping method proposed in this paper has a significant superiority in flexibility of parameters tuning and improvement of vibration suppression, which can be demonstrated in Figs. 10-11, where L is changed from 1 m to 1.5 m and 0.6 m, respectively. Now it is only needed to change ω_1 or ω_2 to tune the time locations of a VI shaper. However, it is not the case if an EI shaper is considered, due to the coupling relationship between ω_d in time locations and V_{tol} in amplitudes of the impulses, which results in a poor flexibility of parameter correction. In addition, according to Table 2, the residual vibration of the VI shaper is obviously smaller than the traditional EI method.

5. CONCLUSION

In this paper, inspired from the two-mode ZV and EI shaper, a new robust VI shaper is proposed. Compared with the existing shapers, the new shaper has the superiorities of good robustness and improved accuracy. In addition, it is more convenient considering the parameter

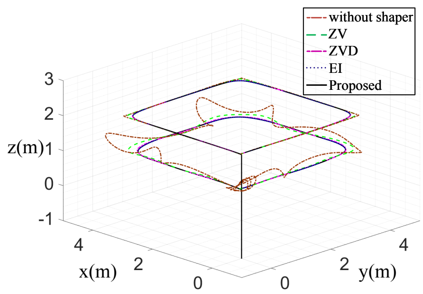

Fig. 7. Comparison results under accurate model

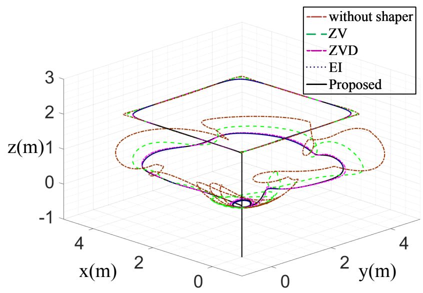

Fig. 8. Results when L is changed from 1 m to 1.5 m

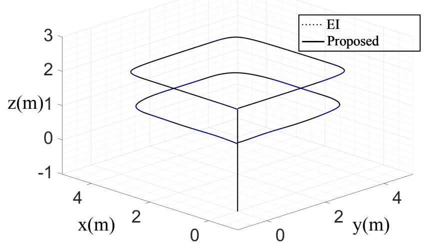

Fig. 9. Comparison result of EI and VI when $L = 1$ m

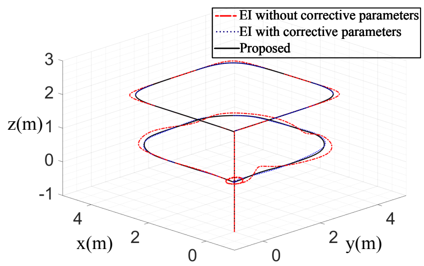

Fig. 10. Comparison result of EI and VI when L is changed to 1.5 m

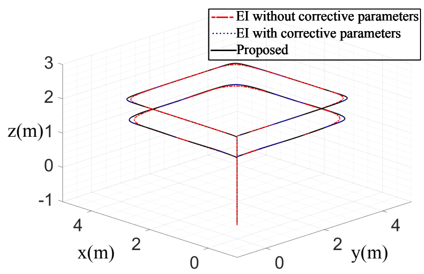

Fig. 11. Comparison result of EI and VI when L is changed to 0.6 m

Table 2. Vibration Comparision

Parameter	Vibration results(rad)		
L(m)	uncorrective EI	corrective EI	VI
1	**0.005**	**0.005**	**0.005**
1.5	0.26	0.05	**0.02**
0.6	0.005	0.005	**0.002**

tuning. Finally, the new command shaper is used in a quadrotor slung system, and its effectiveness and flexibility in design are illustrated by numerical simulations compared with other shapers. In future, this control method will be verified by experimental studies.

REFERENCES

Adams, C., Potter, J., and Singhose, W. (2015). Input-shaping and model-following control of a helicopter carrying a suspended load. *Journal of Guidance, Control, and Dynamics*, 38(1), 94–105.

Auernig, J.W. and Troger, H. (1987). Time optimal control of overhead cranes with hoisting of the load. *Automatica*, 23(4), 437–447.

Haddadi, S.J., Zarafshan, P., and Niroumand, F.J. (2015). Dynamics modelling and implementation of an attitude control on an octorotor. In *IEEE 28th Canadian Conference on Electrical and Computer Engineering (CCECE)*, 722–727.

Huo, X., Chen, J., Liu, Q., and He, X. (2019). Vibration elimination for quadrotor slung system based on input shaping and double closed-loop control. In *12th Asian Control Conference (ASCC)*, 492–497.

Ingram, G. A., F.M.A. and Chiu, G.T.C. (2002). Reducing operator-induced machine vibration using a complex pole/zero prefilter. *Journal of Sound and Vibration*, 250(2), 197–213.

Kim, D. and Singhose, W. (2010). Performance studies of human operators driving double-pendulum bridge cranes. *Control Engineering Practice*, 18(6), 567–576.

Mellinger, D., Michael, N., Shomin, M., and Kumar, V. (2011). Recent advances in quadrotor capabilities. In *2011 IEEE International Conference on Robotics and Automation*, 2964–2965.

Njeri, W., S.M. and Matsushita, K. (2018). Two-degree-of-freedom control of a multilink flexible manipulator using filtered inverse feedforward controller and strain feedback controller. In *IEEE International Conference on Applied System Invention (ICASI)*, 972–975.

Sadr, S., Moosavian, S.A.A., and Zarafshan, P. (2014). Damping control of a quadrotor with swinging load using input shaping method. In *Second RSI/ISM International Conference on Robotics and Mechatronics (ICRoM)*, 227–232.

Singer, N.C. and Seering, W.P. (1990). Preshaping command inputs to reduce system vibration. *Journal of Dynamic Systems, Measurement, and Control*, 112(1), 76–82.

Singhose, W. and Seering, W. (eds.) (2011). *Command Generation For Dynamic Systems*. Atlanta, GA.

Singhose, W. (2009). Command shaping for flexible systems: A review of the first 50 years. *International Journal of Precision Engineering and Manufacturing*, 10(4), 153–168.

Smith, O.J.M. (1957). Posicast control of damped oscillatory systems. *Proceedings of the IRE*, 45(9), 1249–1255.